

Original Article

Antitumor effects of valdecoxib on hypopharyngeal squamous carcinoma cells

Nguyen Thi Kieu Trang^{1,2} and Hoon Yoo^{1,*}

¹Department of Pharmacology and Dental Therapeutics, College of Dentistry, Chosun University, Gwangju 61452, Korea, ²Department of Pharmacy, Thai Binh University of Medicine and Pharmacy, Thai Binh City 06000, Vietnam

ARTICLE INFO

Received February 25, 2022

Revised July 5, 2022

Accepted July 18, 2022

*Correspondence

Hoon Yoo

E-mail: hoon_yoo@chosun.ac.kr

Key Words

Apoptosis

Hypopharyngeal squamous cell carcinoma

Integrin α 4/FAK signaling

MAPK pathway

Valdecoxib

ABSTRACT The antitumoral effects of valdecoxib (Val), an United States Food and Drug Administration-approved anti-inflammatory drug that was withdrawn due to the side effects of increased risk of cardiovascular adverse events, were investigated in hypopharyngeal squamous cell carcinoma cells by performing a cell viability assay, transwell assay, immunofluorescence imaging, and Western blotting. Val markedly inhibited cell viability with an IC50 of 67.3 μ M after 48 h of treatment, and also downregulated cell cycle proteins such as Cdks and their regulatory cyclin units. Cell migration and invasion were severely suppressed by inhibiting integrin α 4/FAK expression. In addition, Val activated the cell cycle checkpoint CHK2 in response to excessive DNA damage, which led to the activation of caspase-3/9 and induced caspase-dependent apoptosis. Furthermore, the signaling cascades of the PI3K/AKT/mTOR and mitogen-activated protein kinase pathways were significantly inhibited by Val treatment. Taken together, our results indicate that Val can be used for the treatment of hypopharyngeal squamous cell carcinoma.

INTRODUCTION

Hypopharyngeal squamous cell carcinoma constitutes 5%–15% of head and neck squamous cell carcinoma (HNSCC) and is the sixth most common cancer in the world. Its prevalence has markedly increased in developing countries, accounting for approximately 20%–35% of all the HNSCC cases reported globally [1,2]. In particular, patients with hypopharyngeal cancer have the worst prognosis among the patients with advanced head and neck cancer and poor five-year survival rates. For example, the five-year survival rate of patients with hypopharynx cancer at stage IV in Taiwan is only 24.8% [3]. Conventional treatment for hypopharyngeal squamous cell carcinoma is a combination of surgery, radiotherapy and chemotherapy, in which concomitant chemoradiotherapy promotes locoregional tumor control and increases survival rates compared to radiotherapy alone.

Valdecoxib (Val) is a nonsteroidal anti-inflammatory drug, which was approved by United States Food and Drug Administration (FDA) for the treatment of inflammatory diseases; however, the drug was withdrawn from the US market in 2005 due to the reported side effects including increased risk of cardiovascular adverse events and serious skin reactions. Recently, antitumor effects of Val and other COX-2 inhibitors (e.g., celecoxib) have been reported as the drugs induced cell proliferation arrest and apoptosis in nasopharyngeal carcinoma cells, and promoted cell lysis in lung cancer cells [4,5]. In addition, combining celecoxib with other therapeutics, such as capecitabine or cyclophosphamide, improved the clinical benefits while reducing the toxicity of monotherapy in metastatic breast cancer [6]. Val also exerted the potential effects of increasing lipid composition, order, and dynamics in colon cancer [7]. Despite these promising reports, the antineoplastic effect and molecular mechanism of action of Val



This is an Open Access article distributed under the terms of the Creative Commons Attribution Non-Commercial License, which permits unrestricted non-commercial use, distribution, and reproduction in any medium, provided the original work is properly cited.
Copyright © Korean J Physiol Pharmacol, pISSN 1226-4512, eISSN 2093-3827

Author contributions: All experiments were conducted by N.T.K.T. under the supervision of Prof. H.Y. Authors have participated in editing and revising the manuscript.

in HNSCC are not well understood. Therefore, we investigated the antitumor activity of Val in FaDu hypopharyngeal squamous carcinoma cells and attempted to elucidate its cellular mechanism of action. Here, we report that Val has antitumor effects on cell cycle regulatory proteins, caspases, integrins, mitogen-activated protein kinase (MAPK) pathway, and PI3K/AKT/mTOR pathway, which lead to the suppression of cell proliferation and mobility, as well as the induction of apoptosis.

METHODS

Antibodies and reagents

Val (purity $\geq 98.0\%$), dimethylsulfoxide (DMSO), diphenyl-eneiodonium (DAPI), 3-(4,5-dimethylthiazol-2-yl)-2,5-diphenyl-tetrazolium bromide (MTT) were purchased from Sigma-Aldrich (St. Louis, MO, USA). Minimum essential medium Eagle (MEM), fetal bovine serum (FBS), trypsin-ethylenediaminetetraacetic acid (EDTA), and antibiotic-antimycotic solution were obtained from Welgene (Daegu, Korea). Primary antibodies against cyclins (A, B1, and E), Cdk2, Cdk4, Cdk7, CDC25C, precursor caspase-3, caspase-9, p-AKT, p-mTOR, MMP1, MMP2, MMP9, fibronectin, VCAM-1, and β -actin were obtained from Santa Cruz Biotechnology (Santa Cruz, CA, USA). The cleaved PARP antibody was purchased from Abcam (Cambridge, MA, USA). Cyclin D1, cleaved caspase-3, p-p42/p44 ERK1/2, p-p38 MAPK1/2, p-JNK, p-H2AX, p-CHK2, p-PI3K, PI3K p85, and integrins were obtained from Cell Signaling Technology (Danvers, MA, USA).

Cell culture

FaDu hypopharyngeal squamous carcinoma cells were grown in MEM, supplemented with 10% FBS and 100 units/ml penicillin/streptomycin at 37°C in a humidified atmosphere with 5% CO₂. The cells (2×10^5 cells/ml) were incubated for 24 h before being treated with various concentrations of Val (0, 25, 50, and 75 μ M).

Cell viability assay

Cell viability was determined using a substrate consisting of MTT. Briefly, the cells were seeded at a density of 4×10^4 cells/well in 96-well plates for 24 h and then treated with various concentrations of Val. After 48 h, the media was removed, and 50 μ l of MTT solution (0.5 mg/ml) was added to each well and incubated for 4 h at 37°C. Upon the formation of violet crystals, the MTT solution was removed and 100 μ l of DMSO was added to dissolve the formazan crystals. The optical density was measured at a wavelength of 540 nm using a Multiskan FC microplate photometer (Thermo Fisher, Waltham, MA, USA).

Wound healing assay

FaDu cells (2×10^5 cells/well) were seeded onto coverslips in a 24-well plate to reach 80% confluence. Using pipette tips, a scratch was made in the middle of the coverslips. The cells were treated with Val (0, 25, 50, and 75 μ M) for 48 h in an incubator. The images of the wounds were captured using a Zeiss AxioScopeA1 microscope (Microscope World, Carlsbad, CA, USA), and the width of wound closure in the captured images was determined using an iSolution software (IMT i-solution Inc., Riverton, UT, USA).

Transwell assay

Transwell assays were performed using 24-well Transwell chambers (pore size: 8 μ m; EMD Millipore, Billerica, MA, USA). Briefly, after treatment with Val for 48 h, cells were collected and suspended in serum-free MEM. For the migration assay, 1×10^4 cells in 200 μ l of serum-free media were seeded onto the upper chambers. For the invasion assay, the membranes were coated with 100 μ l of serum-free MEM containing extracellular matrix (2 μ g/ml) for 2 h at 37°C and 100 μ l of cell suspension was added. In both assays, the lower chambers were filled with 750 μ l of basal MEM and incubated at 37°C. After 24 h, cells on the bottom were washed with PBS and fixed with 4% paraformaldehyde. Cells in the upper compartments were gently removed using cotton swabs, and the cells on the lower side of inserts were stained with 2% crystal violet for 15 min at room temperature. The membranes were then washed with distilled water to remove the stained solution. Images of cells were captured using a Zeiss AxioScopeA1 microscope (Microscope World). These cells were dissolved in 10% cetylpyridinium chloride solution, and the optical density was measured at 590 nm using a Multiskan FC microplate photometer (Thermo Fisher).

Western blotting

FaDu cells (2×10^5 cells/ml) grown in 60 cm plates for 24 h were treated with Val for 48 h. Thereafter, proteins were extracted using lysis buffer (20 mM Tris-HCl pH 7.5, 150 mM NaCl, 1 mM Na₂EDTA, 1 mM EGTA, 1% Triton X-100, 2.5 mM sodium pyrophosphate, 1 mM β -glycerophosphate, 1 mM Na₃VO₄, 1 μ g/ml leupeptin, and 1 mM PMSF) on ice for 30 min. Protein concentration was determined using the Bradford method (Thermo Scientific, Rockford, IL, USA). Total proteins from cell lysates were separated using sodium dodecyl sulfate polyacrylamide gel electrophoresis (SDS-PAGE; 12% resolving gel) and subsequently transferred to nitrocellulose membranes using the Bio-Rad wet blot system (Bio Rad Laboratories, Hercules, CA, USA). After blocking with 5% skimmed milk for 1 h, the membranes were incubated with primary antibodies at 4°C overnight, followed by incubation with HRP-conjugated secondary antibodies for 2 h.

Finally, proteins were detected using chemiluminescent reagents, and images were captured using the Kodak Digital Science Image Station (Bruker BioSpin, Billerica, MA, USA).

Immunofluorescence imaging

FaDu cells (2×10^5 cells/well) seeded onto coverslips were grown in 24-well plates for 24 h and then treated with Val (0, 25, 50, and 75 μM) for 48 h. After washing with PBS, cells were fixed with 4% paraformaldehyde for 15 min at room temperature and then again washed with PBS. The fixed cells were blocked and permeabilized with washing solution (PBS containing 0.1% Triton X-100 and 0.1% goat serum) for 1 h at room temperature. Thereafter, the cells were probed with Cdk1 and p-H2AX antibodies at 4°C overnight. Once washed with washing solution, the cells were incubated with goat anti-mouse Alexa Fluor 488-labeled IgG (1:1,000) (to detect Cdk1), goat anti-rabbit Alexa Fluor 495-labeled IgG (1:1,000) (to detect p-H2AX), and DAPI for 2 h at room temperature. Finally, coverslips were mounted onto microscopic slides and cell images were captured using a fluorescence microscope (Carl Zeiss, Oberkochen, Germany).

RESULTS

Val inhibited FaDu cell viability and downregulated the expression of cell cycle regulating proteins

To investigate the cytotoxicity of Val on FaDu cells, cells were exposed to various concentrations of Val for 48 h. Percent cell viability (determined by MTT assay) was markedly decreased in a dose-dependent manner with an IC₅₀ of 67.3 μM (Fig. 1A). In addition, the expression of various cell cycle regulators, such as

cyclin A, B1, D1, E, Cdk1, Cdk2, and Cdk4 was downregulated by Val treatment in a dose-dependent manner (Fig. 1B). In particular, Cdk1 expression was severely reduced at a dose of 75 μM .

Val suppressed cell migration and invasion

The effect of Val on cell mobility was investigated using wound healing and transwell assays. Val effectively inhibited FaDu cell migration and invasion in a dose-dependent manner (Fig. 2). At a concentration of 50 μM , both cell migration and invasion dropped to approximately 40% of the initial values, indicating that Val significantly suppressed cell mobility.

Val suppressed the integrin α 4/FAK signaling pathway

The integrin family plays a crucial role in cell migration and invasion by interacting with the extracellular matrix. Among the integrins and regulators of the integrin pathway, the expression of integrin alpha 4 (ITGA4) was significantly suppressed at 75 μM Val, whereas the expressions of integrin α 5 and α v were moderately suppressed (Fig. 3A). The activated form of downstream phosphorylated-FAK (p-FAK) was notably downregulated at 75 μM Val while maintaining the total form of total-FAK (t-FAK). Val also inhibits the expression of matrix metalloproteinases (MMP1, MMP2, and MMP9), which are responsible for the degradation of collagen and gelatin. However, the expression levels of VCAM-1 and fibronectin, which are typical substrates of ITGA4, were elevated (Fig. 3B).

Val induced caspase-dependent apoptosis

Western blotting analysis revealed that Val significantly in-

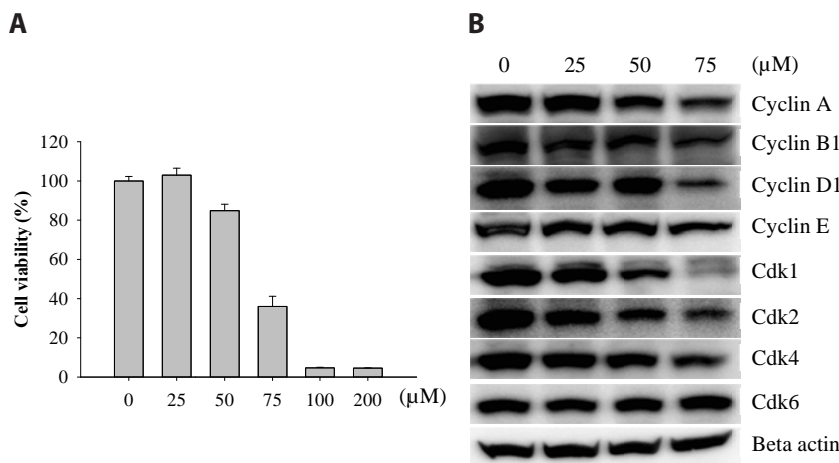


Fig. 1. Valdecoxib (Val) inhibited cell proliferation and cell cycle protein expression. FaDu cells were treated with various concentrations of Val for 48 h, and MTT assay was performed to measure the percent cell viability (A). Cells were treated with 0, 25, 50, and 75 μM of Val for 48 h, and total proteins were extracted. Various antibodies were used to detect Cyclins and Cdks (B). Vertical bars indicate means and standard errors ($n = 3$). MTT, 3-(4,5-dimethylthiazol-2-yl)-2,5-diphenyltetrazolium bromide.

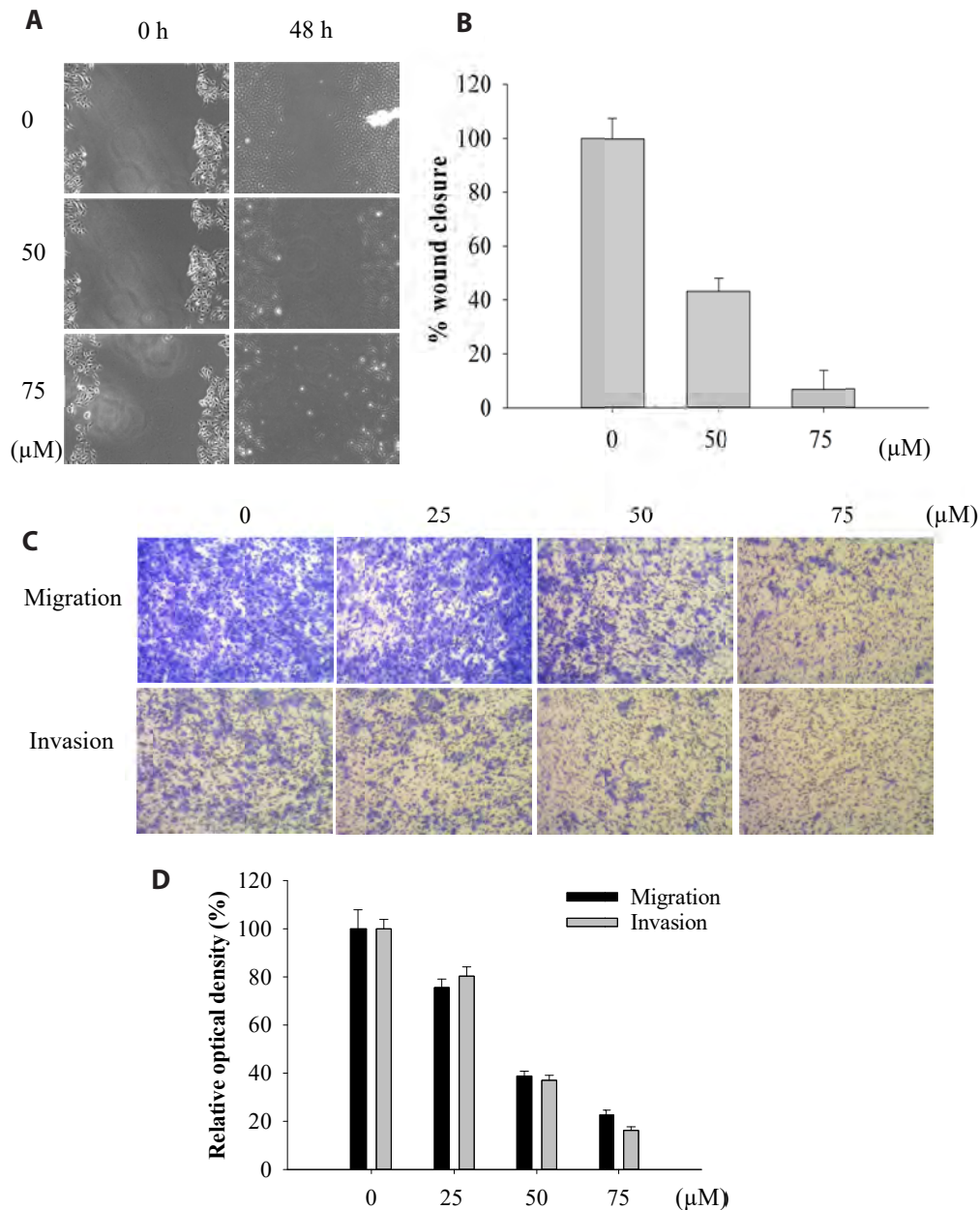


Fig. 2. Valdecoxib (Val) inhibited FaDu cell migration and invasion. FaDu cells were seeded onto coverslips in 24-well plates for 24 h. After cells reached 80% confluence, a scratch (5 mm) was made with a 10 μ l pipette tip, and then cells were treated with Val (0, 50, and 75 μ M) for 48 h. Images of the wound were taken using a microscope (A: \times 100, magnification) and the degree of wound closure was measured (B). The transwell assay was performed to identify the migrating and invading cells using 8 μ m cell hanging inserts. Cells were stained with crystal violet and images were captured using a microscope (C: \times 100 magnification). To quantify the percentage of migrated and invaded cells, they were dissolved in 10% cetylpyridinium chloride and the optical density was recorded using a microplate photometer (D). Vertical bars indicate means and standard errors ($n = 3$).

duced the activation of caspase-9, caspase-3, and PARP. The concentrations of cleaved forms of caspase-9 and caspase-3 increased in a dose-dependent manner after Val treatment, while the concentrations of precursor forms decreased. In addition, the expression of cleaved PARP (89 kDa) was increased by the action of caspases on PARP (Fig. 4), suggesting that Val induced caspase-dependent apoptosis.

Val induced cell cycle checkpoint 2 (p-CHK2) activation

The effect of Val on DNA damage was examined using immunofluorescence (Fig. 5A) and Western blotting (Fig. 5B). p-H2AX and p-CHK2, key marker proteins that respond to DNA damage, were overexpressed in the chromosomes of Val-treated FaDu cells. In addition, the expression of cell division cycle 25C

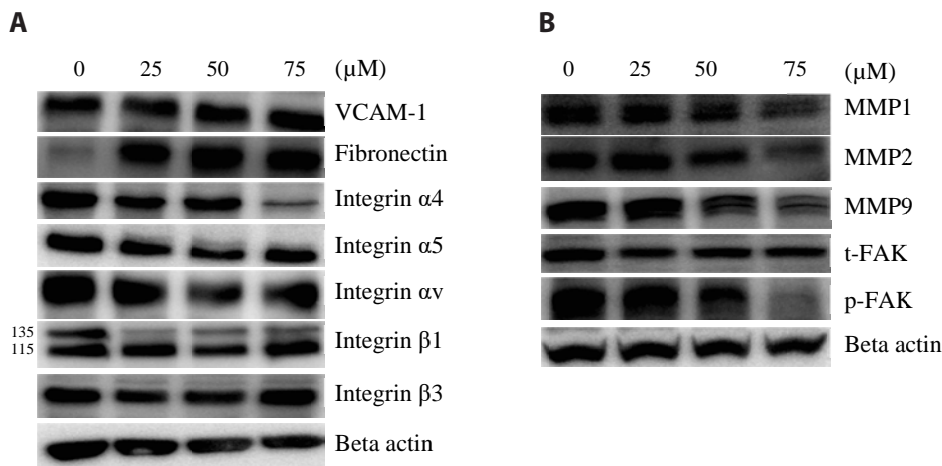


Fig. 3. Valdecoxib (Val) regulated the MMP/integrin α 4/FAK pathway in FaDu cells. Cells were treated with 0–75 μ M of Val for 48 h, followed by total protein extraction. Proteins were separated by SDS-PAGE and primary antibodies against VCAM-1, fibronectin, integrins (A), MMPs, total-FAK (t-FAK), and phosphorylated-FAK (p-FAK) were used to detect these proteins (B).

(CDC25C), an important phosphatase for checkpoint regulation, rapidly decreased in response to DNA damage.

Val suppressed the PI3K/AKT/mTOR and MAPK pathways

Val treatment strongly inhibited the PI3K/AKT/mTOR and MAPK cascades, which play significant roles in the regulation of cell survival, proliferation, and apoptosis. Western blotting results showed that the expression or activation of the various key regulators of the PI3K/AKT/mTOR (PI3K p85, p-PI3K, and p-mTOR) and MAPK pathway (p-JNK, p-ERK, and p-p38) were suppressed in a dose-dependent manner, particularly at 75 μ M Val concentration (Fig. 6). Together with our earlier results of the reduced expression of cell cycle proteins and activated caspases, this observation supported the hypothesis that proliferation was suppressed and apoptosis was induced partly through the inhibitory action of Val on the PI3K/AKT/mTOR and MAPK pathways.

DISCUSSION

In this study, we investigated the anti-cancer activity of Val in hypopharyngeal squamous cell carcinoma using FaDu cells. Val inhibited cell proliferation in a dose-dependent manner and induced apoptosis through regulation of the CHK2/CDC25C/Cdk1 pathway. Various cell cycle regulatory proteins such as cyclins and Cdks were downregulated, including Cdk1, an archetypical kinase that plays an essential role in driving cells through the G2/M phase transition [8]. The cyclin B1/Cdk1 complex translocates into the nucleus and activates a range of target proteins, which assist in transitioning of cell from interphase to mitotic phase [9]. After Val treatment, the expression of both Cdk1 and cyclin B1 was significantly suppressed (Fig. 1), and DNA damage was followed by increased expression of p-H2AX in the nucleus (Fig. 5). The expression of CHK2, in response to DNA damage, negatively controls Cdk1 through CDC25 or p53 to repair the damaged

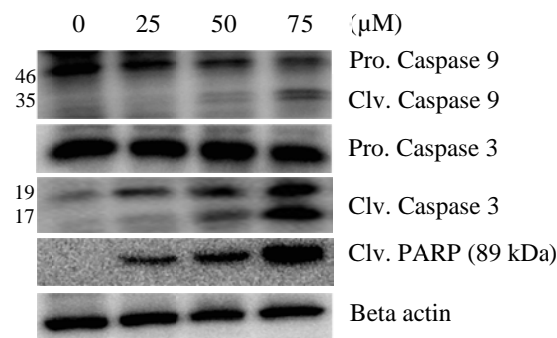


Fig. 4. Valdecoxib (Val) induced apoptosis through the activation of caspases. FaDu cells were treated with Val (0, 25, 50, and 75 μ M) for 48 h, and the precursor/cleaved forms of caspase-3, caspase-9, and PARP (89 kDa) were detected using Western blotting.

DNA before entering mitosis. In this study, excessive augmentation of activated p-CHK2 under Val treatment and the corresponding decrease in CDC25C and Cdk1 expressions, which did not affect p53 expression, supported the hypothesis that Val suppressed FaDu cell proliferation through CHK2/CDC25C/Cdk1 signaling and that cell cycle arrest was p53-independent (Fig. 5). The activation of CHK2 might have caused the phosphorylation and degradation of CDC25C, thus preventing the activation of downstream Cdk1 and cyclin B1 for the G2/M phase transition. Furthermore, Val-induced superabundant DNA damage outweighed the repair capacity of the cells, leading to programmed cell death through the activation of caspases (cleaved caspases-3 and -9) (Fig. 4).

Val effectively inhibited tumor cell migration and invasion by downregulating the ITGA4/FAK pathway (Fig. 2). Integrins are cell adhesion receptors that play important roles in cell signaling between the internal cytoskeletal network and extracellular environment [10]. Among the integrins examined, ITGA4 was the most significantly suppressed by Val, especially at 75 μ M concentration, while other integrins were moderately inhibited or unchanged. The relationship between ITGA4 and tumor aggressiveness has been reported for various types of cancers [11]. Ele-

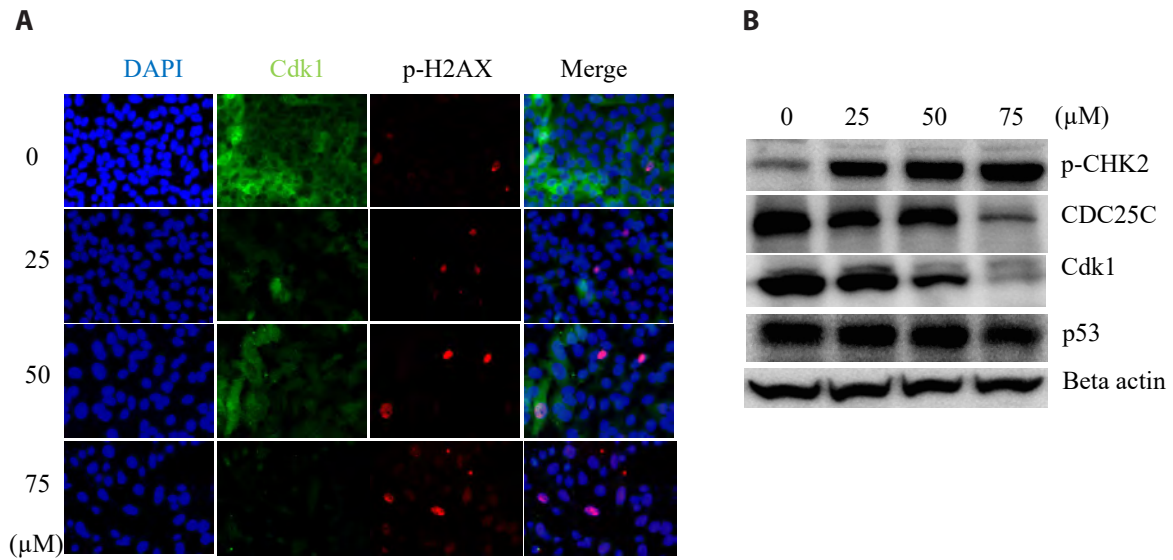


Fig. 5. Valdecoxib (Val) induced DNA double-strand breaks and CHK2 activation. After Val treatment of FaDu cells, the localization and expression of Cdk1 and p-H2AX were examined using immunofluorescence imaging after staining with specific antibodies. The images were captured using a fluorescent microscope at 400x magnification (A). The expressions of p-CHK2, p53, and CDC25C were examined using Western blotting (B).

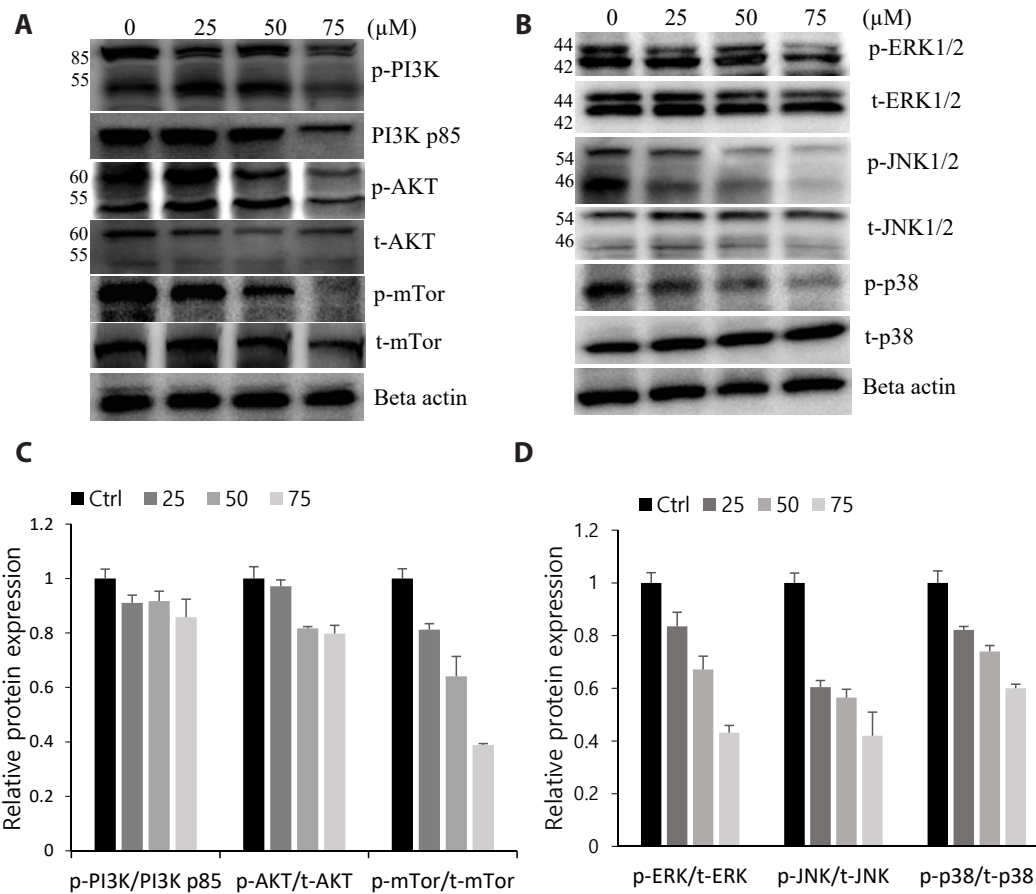


Fig. 6. Valdecoxib (Val) inhibited the PI3K/AKT/mTOR and MAPK pathways. Cells were treated with various concentrations of Val for 48 h. Total proteins were extracted and separated using SDS-PAGE. Antibodies against PI3K p85, p-PI3K, p-AKT, and p-mTOR were used to detect the expression of corresponding proteins (A, B) and the relative phosphorylation level was quantified (C, D). Vertical bars indicate means and standard errors (n = 3). MAPK, mitogen-activated protein kinase.

vated expression of ITGA4 using specific substrates increases cell mobility in neuroblastoma, and an association between ITGA4 levels and tumor aggressiveness has been found in clinical cases [12]. In addition, suppression of integrin $\alpha 4\beta 1$ upregulates the efficacy of chemotherapy in ovarian cancer [13]. In gastrointestinal stromal tumors, ITGA4 expression is associated with adverse prognostic features and survival rates [14]. Notably, in our study, the expression of fibronectin and VCAM-1, extracellular matrix ligands that bind and regulate integrin signaling pathways, was considerably increased under Val treatment. This might be due to the compensatory action of FaDu cells to make effective use of the reduced expression of ITGA4 receptors under Val treatment. At high doses of Val, severe loss of ITGA4 receptors might have disrupted cell-cell and cell-extracellular matrix adhesion, leading to a subsequent decrease in downstream p-FAK (Fig. 3). In addition, decreased expression of matrix metalloproteinases (MMP1, MMP2, and MMP9) following Val treatment suppressed cell mobility and restricted tumor growth and invasion.

Val downregulated the key regulators of the PI3K/AKT/mTOR and MAPK cascades, supporting the suppression of proliferation, mobility, and apoptosis induction. The PI3K/AKT/mTOR pathway is over-activated in approximately 60% of HNSCC cases, and a crosstalk between the PI3K/AKT/mTOR and MAPK pathways has also reported [15]. Thus, inhibiting a pivotal intracellular cascade or cotargeting both pathways could be crucial for HNSCC treatment [16], as well as other cancers [17,18]. In conclusion, we confirmed that Val has antitumor effects on hypopharyngeal squamous cell carcinoma by suppressing cell proliferation and mobility, and inducing apoptosis. Our results support that Val could be a potential candidate for treating hypopharyngeal squamous cell carcinoma.

FUNDING

This study was supported by research funds from Chosun University (2021).

ACKNOWLEDGEMENTS

None.

CONFLICTS OF INTEREST

The authors declare no conflicts of interest.

REFERENCES

- Lu W, Feng L, Li P, Wang Y, Du Y, Chen X, Wu S, Zhao G, Lou W. Effects of HPV-16 infection on hypopharyngeal squamous cell carcinoma and FaDu cells. *Oncol Rep.* 2016;35:99-106.
- Gupta T, Chopra S, Agarwal JP, Laskar SG, D'cruz AK, Shrivastava SK, Dinshaw KA. Squamous cell carcinoma of the hypopharynx: single-institution outcome analysis of a large cohort of patients treated with primary non-surgical approaches. *Acta Oncol.* 2009;48:541-548.
- Chang MF, Wang HM, Kang CJ, Huang SF, Lin CY, Fang KH, Chen EY, Chen IH, Liao CT, Chang JT. Treatment results for hypopharyngeal cancer by different treatment strategies and its secondary primary--an experience in Taiwan. *Radiat Oncol.* 2010;5:91.
- Liu DB, Hu GY, Long GX, Qiu H, Mei Q, Hu GQ. Celecoxib induces apoptosis and cell-cycle arrest in nasopharyngeal carcinoma cell lines via inhibition of STAT3 phosphorylation. *Acta Pharmacol Sin.* 2012;33:682-690. Erratum in: *Acta Pharmacol Sin.* 2013;34:581.
- Schellhorn M, Hausteiner M, Frank M, Linnebacher M, Hinze B. Celecoxib increases lung cancer cell lysis by lymphokine-activated killer cells via upregulation of ICAM-1. *Oncotarget.* 2015;6:39342-39356.
- Li J, Hao Q, Cao W, Vadgama JV, Wu Y. Celecoxib in breast cancer prevention and therapy. *Cancer Manag Res.* 2018;10:4653-4667.
- Inan Genç A, Gok S, Banerjee S, Severcan F. Valdecoxib recovers the lipid composition, order and dynamics in colon cancer cell lines independent of COX-2 expression: an ATR-FTIR spectroscopy study. *Appl Spectrosc.* 2017;71:105-117.
- Diril MK, Ratnacaram CK, Padmakumar VC, Du T, Wasser M, Coppola V, Tessarollo L, Kaldis P. Cyclin-dependent kinase 1 (Cdk1) is essential for cell division and suppression of DNA re-replication but not for liver regeneration. *Proc Natl Acad Sci U S A.* 2012;109:3826-3831.
- Lindqvist A. Cyclin B-Cdk1 activates its own pump to get into the nucleus. *J Cell Biol.* 2010;189:197-199.
- Qian F, Vaux DL, Weissman IL. Expression of the integrin alpha 4 beta 1 on melanoma cells can inhibit the invasive stage of metastasis formation. *Cell.* 1994;77:335-347.
- Wu L, Bernard-Trifilo JA, Lim Y, Lim ST, Mitra SK, Uryu S, Chen M, Pallen CJ, Cheung NK, Mikolon D, Mielgo A, Stupack DG, Schlaepfer DD. Distinct FAK-Src activation events promote alpha5beta1 and alpha4beta1 integrin-stimulated neuroblastoma cell motility. *Oncogene.* 2008;27:1439-1448.
- Young SA, McCabe KE, Bartakova A, Delaney J, Pizzo DP, Newbury RO, Varner JA, Schlaepfer DD, Stupack DG. Integrin $\alpha 4$ enhances metastasis and may be associated with poor prognosis in MYCN-low neuroblastoma. *PLoS One.* 2015;10:e0120815.
- Scalici JM, Harrer C, Allen A, Jazaeri A, Atkins KA, McLachlan KR, Slack-Davis JK. Inhibition of $\alpha 4\beta 1$ integrin increases ovarian cancer response to carboplatin. *Gynecol Oncol.* 2014;132:455-461.
- Pulkka OP, Mpindi JP, Tynnenen O, Nilsson B, Kallioniemi O, Sihto H, Joensuu H. Clinical relevance of integrin alpha 4 in gastrointestinal stromal tumours. *J Cell Mol Med.* 2018;22:2220-2230.
- Rieke DT, Klinghammer K, Keilholz U. Targeted therapy of head and neck cancer. *Oncol Res Treat.* 2016;39:780-786.
- Massacesi C, Di Tomaso E, Urban P, Germa C, Quadt C, Trandafir L, Aimone P, Fretault N, Dharan B, Tavorath R, Hirawat S. PI3K inhibitors as new cancer therapeutics: implications for clinical trial design. *Onco Targets Ther.* 2016;9:203-210.
- Renshaw J, Taylor KR, Bishop R, Valenti M, De Haven Brandon A, Gowan S, Eccles SA, Ruddle RR, Johnson LD, Raynaud FI, Selve JL.

- Thway K, Pietsch T, Pearson AD, Shipley J. Dual blockade of the PI3K/AKT/mTOR (AZD8055) and RAS/MEK/ERK (AZD6244) pathways synergistically inhibits rhabdomyosarcoma cell growth in vitro and in vivo. *Clin Cancer Res*. 2013;19:5940-5951.
18. Peng X, Liu Y, Zhu S, Peng X, Li H, Jiao W, Lin P, Zhang Z, Qiu Y, Jin M, Wang R, Kong D. Co-targeting PI3K/Akt and MAPK/ERK pathways leads to an enhanced antitumor effect on human hypopharyngeal squamous cell carcinoma. *J Cancer Res Clin Oncol*. 2019;145:2921-2936.